Synthesis of Eu^{3+}/Yb^{3+} Co-Doped $LiY(MoO_4)_2$ Particles via Microwave Sol-Gel Route and their Upconversion and Spectroscopic Properties

Chang Sung Lim

Department of Advanced Materials Science & Engineering, Hanseo University, Seosan 356-706, Republic of Korea

Abstract: Eu^{3+}/Yb^{3+} co-doped $LiY_{1-x}(MoO_4)_2$ double molybdate phosphors with the correct doping concentrations of Eu^{3+} and Yb^{3+} ($x = Eu^{3+} + Yb^{3+}$, $Eu^{3+} = 0.05$, 0.1, 0.2 and $Yb^{3+} = 0.2$, 0.45) were successfully synthesized via microwave sol-gel route and their upconversion and spectroscopic properties were investigated. The microstructure of the synthesized particles showed a well-crystallized morphology with particle sizes of 2-10 μm. Under excitation at 980 nm, $LiY_{0.5}(MoO_4)_2:Eu_{0.05}/Yb_{0.45}$ particles provided a strong 525-nm and a weak 525-nm emission bands in the green region, and a very weak 615-nm emission band in the red region. The Raman spectra of the doped particles indicated the domination of strong peaks at higher frequencies of 666, 720, 820, 868, 947, and 996 cm^{-1} and weak peaks at lower frequencies of 294, 338 and 358 cm^{-1} induced by the disorder of the $[MoO_4]^{2-}$ groups with the partial substitution of Y^{3+} by Eu^{3+} and Yb^{3+} ions into the $LiY_{1-x}(MoO_4)_2$ crystal lattice, which resulted in the highly modulated structure as well as a concentration quenching effect of Eu^{3+} ions.

Key words: $LiY(MoO_4)_2$: Eu^{3+}/Yb^{3+}, Microwave sol-gel, Upconversion photoluminescence, Raman spectroscopy.

Introduction

Double molybdates doped with lanthanide ions with the formular of $MR(MoO_4)_2$ ($M = Li^+$, Na^+, K^+; $R = La^{3+}$, Gd^{3+}, Y^{3+}) have attracted great interest in the recent years [1]. Their structural variation of these double molybdates provides unique physical and chemical properties for the possibility of doping with lanthanide ions, and wide range of applications, such as cathode ray tubes, fluorescent lamps, solid-state laser, amplifiers for fiber optics and new optoelectronic devices. It shows highly luminescent quantum yields, since usually more than one metastable excited state exists, and multiple emissions are detected [2,3]. Double molybdates with a sheelite-type structure have been of practical interest due to their attractive spectroscopic characteristics showing potential application as photoluminescent phosphors and scintillators. For the trivalent lanthanide ions in the disordered tetragonal-phase, it is possible to be partially substituted by Eu^{3+} and Yb^{3+} ions; these ions are effectively

Corresponding author: *cslim@hanseo.ac.kr*

doped into the crystal lattices of the tetragonal phase due to the similar radii of the trivalent lanthanide ions in R^{3+}, which lead to the excellent upconcersion (UC) photoluminescence properties [4-6].

The $[MoO_4]^{2-}$ group has strong absorption in the near ultraviolet region, so that the energy transfer process from the $[MoO_4]^{2-}$ group to the rare earth ions can easily occur, which can greatly enhance the external quantum efficiency of rare-earth ion doped materials. Among lanthanide ions, the Eu^{3+} ion as an activator and Yb^{3+} ion as a sensitizer are suitable for converting infrared to visible light through the UC process due to its appropriate electronic energy level. The co-doped system of Eu^{3+} ion and Yb^{3+} ion can remarkably enhance the UC efficiency for the shift from infrared to visible light due to the highly effective efficiency of the energy transfer (ET) from Yb^{3+} to Eu^{3+}. The Yb^{3+} ion, as a sensitizer, can be effectively excited by an incident light source energy. This energy is transferred to the activator of Eu^{3+} ion from which radiation can be emitted [7-9].

To prepare the lanthanide doped double molybdates, several processes have been developed for specific purposes [10-15]. Usually, the sol-gel method provides some advantages over the conventional solid-state method, showing good homogeneity, low calcination temperature, small particle size and narrow particle size distribution optimal. However, the sol-gel method has a disadvantage in that it takes a long time for gelation. Microwave sol-gel synthesis has the advantages of very short synthesis time, homogeneous morphology features and high purity of final polycrystalline samples [16-18]. Microwave heating energy is transferred to the material surface generated via radiant and/or convection heating, which heat energy is delivered to the bulk of the material by conduction [19,20]. Especially, microwave sol-gel process is a highly effective method to provide high homogeneity and high purity of final products with a convenient process; it is a representative method as a viable new approach for the synthesis of high-quality luminescent materials. However, synthesis of Eu^{3+}/Yb^{3+} co-doped $LiY(MoO_4)_2$ phosphors via the microwave sol-gel route has not yet been reported.

In this study, Eu^{3+}/Yb^{3+} co-doped $LiY(MoO_4)_2$ phosphors with the correct doping concentrations of Eu^{3+} and Yb^{3+} ($x = Eu^{3+} + Yb^{3+}$, $Eu^{3+} = 0.05$, 0.1, 0.2 and $Yb^{3+} = 0.2$, 0.45) phosphors were prepared via the microwave sol-gel route. The characterization of the synthesized particles were evaluated by X-ray diffraction (XRD), scanning electron microscopy (SEM). The upconversion and spectroscopic properties were investigated comparatively using photoluminescence (PL) emission and Raman spectroscopy.

Experimental

Fig. 1 provides a flow chart for the synthesis of Eu^{3+}/Yb^{3+} co-doped $LiY(MoO_4)_2$ phosphors. Appropriate stoichiometric amounts of $HLiO{\cdot}H_2O$ (99%, Sigma-Aldrich, USA), $Y(NO_3)_3{\cdot}6H_2O$ (99 %, Sigma-Aldrich, USA), $(NH_4)_6Mo_7O_{24}{\cdot}4H_2O$ (99%, Alfa Aesar, USA), $Eu(NO_3)_3{\cdot}5H_2O$ (99.9%, Sigma-Aldrich, USA), $Yb(NO_3)_3{\cdot}5H_2O$ (99.9%, Sigma-Aldrich, USA), citric acid (99.5%, Daejung Chemicals, Korea), NH_4OH (A.R.), ethylene glycol (A.R.) and distilled

water were used to prepare $LiY(MoO_4)_2$, $LiY_{0.8}(MoO_4)_2:Eu_{0.2}$, $LiY_{0.7}(MoO_4)_2:Eu_{0.1}Yb_{0.2}$ and $LiY_{0.5}(MoO_4)_2:Eu_{0.05}Yb_{0.45}$ compounds with the correct doping concentrations of Eu^{3+} and Yb^{3+} (Eu^{3+} = 0.05, 0.1, 0.2 and Yb^{3+}= 0.2, 0.45). To prepare $LiY(MoO_4)_2$, 0.2 mol% $HLiO{\cdot}H_2O$ and 0.114 mol% $(NH_4)_6Mo_7O_{24}{\cdot}4H_2O$ were dissolved in 20 mL of ethylene glycol and 80 mL of 5M NH_4OH with vigorous stirring and heating. Subsequently, 0.4 mol% $Y(NO_3)_3{\cdot}6H_2O$ and citric acid (with a molar ratio of citric acid to total metal ions of 2:1) were dissolved in 100 mL of distilled water under vigorous stirring and heating. Then, the solutions were mixed together under vigorous stirring and heating at 80-100°C. Finally, highly transparent solutions were obtained and adjusted to pH=7-8 by the addition of NH_4OH or citric acid. In order to prepare $LiY_{0.8}(MoO_4)_2:Eu_{0.2}$, the mixture of 0.32 mol% $Y(NO_3)_3{\cdot}6H_2O$ with 0.08 mol% $Eu(NO_3)_3{\cdot}5H_2O$ was used for the creation of the rare earth solution. In order to prepare $LiY_{0.7}(MoO_4)_2:Eu_{0.1}Yb_{0.2}$, the mixture of 0.28 mol% $Y(NO_3)_3{\cdot}6H_2O$ with 0.04 mol% $Eu(NO_3)_3{\cdot}5H_2O$ and 0.08 mol% $Yb(NO_3)_3{\cdot}5H_2O$ was used for the creation of the rare earth solution. In order to prepare $LiY_{0.5}(MoO_4)_2:Eu_{0.05}Yb_{0.45}$, the rare earth containing solution was generated using 0.2 mol% $Y(NO_3)_3{\cdot}6H_2O$ with 0.02 mol% $Eu(NO_3)_3{\cdot}5H_2O$ and 0.18 mol% $Yb(NO_3)_3{\cdot}5H_2O$.

The transparent solutions were located into a microwave oven operating with a frequency of 2.45 GHz for a maximum output-power of 1250 W for 30 min. The working cycle of the microwave process was precisely controlled using a regime of 40 s on and 20 s off for 15 min, and further treated for a regime of 30 s on and 30 s off for 15 min. The samples were treated under ultrasonic radiation for 10 min to produce a light yellow transparent sol. After this, the light yellow transparent sols were dried at 120°C in a dry oven to obtain black dried gels. The black dried gels were ground and heat-treated at 900°C for 16 h with 100°C intervals between 600-900°C. Finally, white particles were obtained for $LiY(MoO_4)_2$ and pink particles were obtained for the Eu^{3+}/Yb^{3+} co-doped $LiY(MoO_4)_2$.

The phase identification of the synthesized particles was evaluated using XRD (D/MAX 2200, Rigaku, Japan). The crystallized microstructure and surface morphology of the synthesized particles were observed using SEM (JSM-5600, JEOL, Japan). The PL spectra were measured using a spectrophotometer (Perkin Elmer LS55, UK) at room temperature. Raman spectroscopic properties were investigated using a LabRam Aramis (Horiba Jobin-Yvon, France) with the spectral resolution of 2 cm^{-1}. The 514.5-nm line of an Ar ion laser was used as an excitation source; the power on the samples was kept at 0.5 mW level to avoid the sample decomposition.

Results and Discussion

Fig. 2 shows the X-ray diffraction patterns of the synthesized (a) $LiY(MoO_4)_2$, (b) $LiY_{0.8}(MoO_4)_2:Eu_{0.2}$, (c) $LiY_{0.7}(MoO_4)_2:Eu_{0.1}Yb_{0.2}$, and (d) $LiY_{0.5}(MoO_4)_2:Eu_{0.05}Yb_{0.45}$ particles. The diffraction patterns of the synthesized particles can be mostly identified with the standard data of $LiY(MoO_4)_2$ (JCPDS 33-0838). $LiY(MoO_4)_2$ as a member of double molybdate family has a sheelite structure, which is tetragonal with a space group $I4_{1/a}$ [21]. The impurity peaks were detected at several degrees. The foreign impurity phases could be detected

when the doping concentration of co-doped Eu^{3+}/Yb^{3+} is 0.05/0.45 mol%. The secondary phases are assumed to be one of the MoO_{4-x} groups (MoO_3, Mo_4O_{11}, Mo_8O_{23} and Mo_9O_{26}). However, it is very difficult to identify the secondary phases because very weak peaks are observed, and the MoO_{4-x} has very similar and complicated reflexes. As to the previous studies, similar impurity phases were also detected in the case of Er^{3+}/Yb^{3+} doped $CaMoO_4$ and $SrMoO_4$ phosphors when the doping concentration of co-doped Er^{3+}/Yb^{3+} is 0.02/0.18 mol% [17,18]. Post heat-treatment provides an important result in a well-defined crystallized morphology. To achieve a well-defined crystalline morphology, the phases are required to be heat treated at 900°C for 16 h. It should be noted that the doping amount of Eu^{3+}/Yb^{3+} provides a great effect on the crystalline cell volume of the $LiY(MoO_4)_2$, because of the different ionic sizes. The co-doped system of Eu^{3+} ion and Yb^{3+} ion can remarkably enhance the UC efficiency due to the highly effective efficiency of the energy transfer (ET) from Yb^{3+} to Eu^{3+}. It should be emphasized that that the synthesized Eu^{3+}/Yb^{3+} co-doped $LiY(MoO_4)_2$ with a tetragonal-phase after partial substitution of Y^{3+} and by Eu^{3+} and Yb^{3+} ions and that the ions are effectively doped into the $LiY(MoO_4)_2$ crystal lattice because of the similar radii of Y^{3+}, Eu^{3+} and Yb^{3+}.

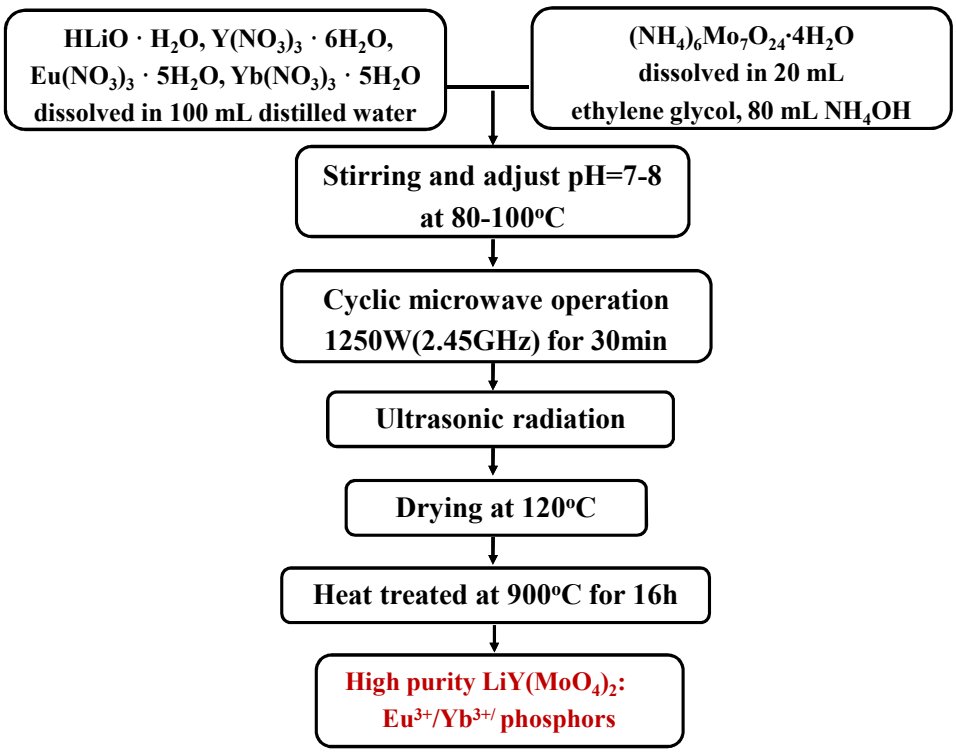

Figure 1: Flow chart for the synthesis of $LiY_{1-x}(MoO_4)_2$:Eu^{3+}/Yb^3 phosphors.

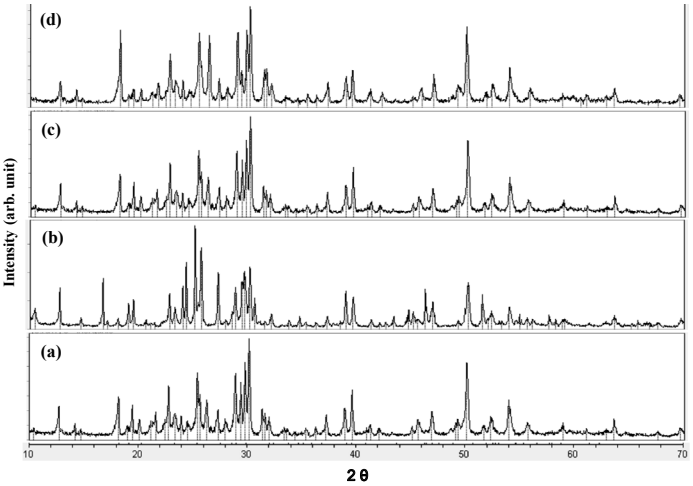

Figure 2: X-ray diffraction patterns of the synthesized (a) $LiY(MoO_4)_2$, (b) $LiY_{0.8}(MoO_4)_2:Eu_{0.2}$, (c) $LiY_{0.7}(MoO_4)_2:Eu_{0.1}Yb_{0.2}$, and (d) $LiY_{0.5}(MoO_4)_2:Eu_{0.05}Yb_{0.45}$ particles.

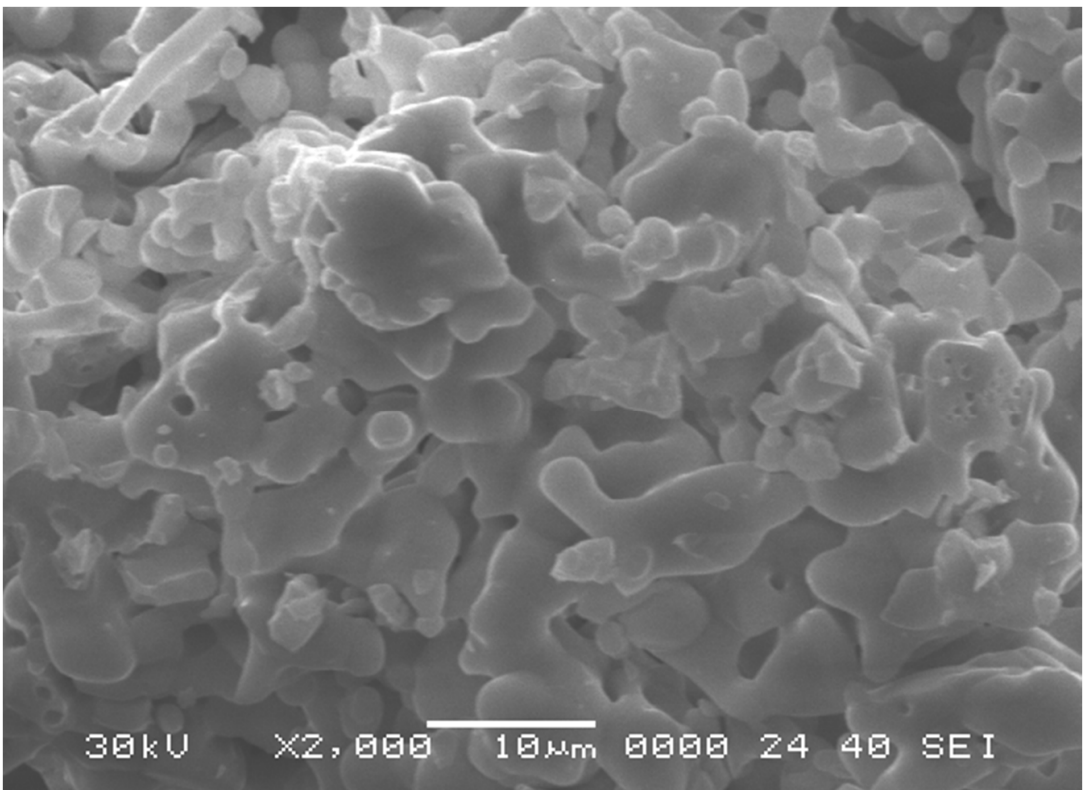

Figure 3: Scanning electron microscopy image of the synthesized $LiY_{0.5}(MoO_4)_2:Eu_{0.05}Yb_{0.45}$ particles.

Fig. 3 shows a SEM image of the synthesized $Eu_{0.05}/Yb_{0.45}$ co-doped $LiY_{0.5}(MoO_4)_2$ particles. The synthesized sample shows well crystallized morphology with particle sizes of 2-10 μm. It should be noted that the doping concentrations for Eu^{3+} and Yb^{3+} have no effects on the morphological feature. The microwave sol-gel method of the double molybdate provides the energy to synthesize the bulk of the material uniformly, so that fine particles with controlled morphology can be fabricated in a short time period. This method is a cost-effective way to fabricate highly homogeneous products and is easy to scale-up; it is a viable alternative for the rapid synthesis of UC particles. This suggests that the microwave sol-gel route is suitable for the growth of $LiY_{1-x}(MoO_4)_2:Eu^{3+}/Yb^{3+}$ crystallites.

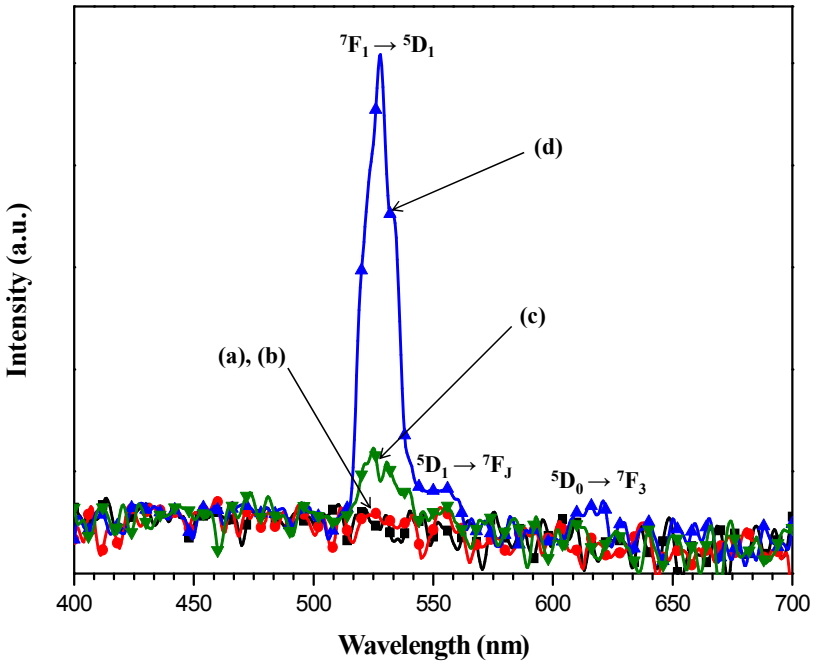

Figure 4: Upconversion photoluminescence emission spectra of (a) $LiY(MoO_4)_2$, (b) $LiY_{0.8}(MoO_4)_2:Eu_{0.2}$, (c) $LiY_{0.7}(MoO_4)_2:Eu_{0.1}Yb_{0.2}$, and (d) $LiY_{0.5}(MoO_4)_2:Eu_{0.05}Yb_{0.45}$ particles excited under 980 nm at room temperature.

Fig. 4 shows the UC photoluminescence emission spectra of (a) $LiY(MoO_4)_2$, (b) $LiY_{0.8}(MoO_4)_2:Eu_{0.2}$, (c) $LiY_{0.7}(MoO_4)_2:Eu_{0.1}Yb_{0.2}$, and (d) $LiY_{0.5}(MoO_4)_2:Eu_{0.05}Yb_{0.45}$ particles excited under 980 nm at room temperature. The UC (d) $LiY_{0.5}(MoO_4)_2:Eu_{0.05}Yb_{0.45}$ particles showed a strong 525-nm and a weak 550 emission bands in the green region, and a very weak 615-nm emission band in the red region. The UC (a) $LiY(MoO_4)_2$, and (b) $LiY_{0.8}(MoO_4)_2:Eu_{0.2}$ were not detected, and the UC (c) $LiY_{0.7}(MoO_4)_2:Eu_{0.1}Yb_{0.2}$ were detected as a weak 525-nm emission band in the green region. The strong 525-nm emission in the green region was assigned to the $^7F_0 \circledcirc {}^5D_1$ transition and the weak emission 550-nm band

in the green region was assigned to the $^5D_1 \rightarrow {}^7F_J$ transition, while the very weak emission 615-nm band in the red region assigns to the $^5D_0 \rightarrow {}^7F_2$ transition [22,23]. The UC intensity of (d) $LiY_{0.5}(MoO_4)_2:Eu_{0.05}Yb_{0.45}$ is much higher than that of (c) $LiY_{0.7}(MoO_4)_2:Eu_{0.1}Yb_{0.2}$ particles. The doping amounts of Eu^{3+}/Yb^{3+} were affected on the crystallized morphology of the phosphors and their UC photoluminescent intensity. The Eu^{3+} ion activator is the luminescence center of these UC particles, and the sensitizer Yb^{3+} effectively enhances the UC luminescence intensity because of the efficient energy transfer from Yb^{3+} to Eu^{3+}. The concentration quenching effect can be explained by the energy transfer between nearest Eu^{3+} and Yb^{3+} ions. With increasing Eu^{3+} and Yb^{3+} ion concentrations, the distance between Eu^{3+} and Yb^{3+} ions decrease, which can promote non-radiative energy transfer such as an exchange interaction or multipole-multipole interactions [25]. The concentration quenching of upconversion emissions could be mainly attributed to the different doping ions. As shown in Fig. 4, the higher intensity of (d) $LiY_{0.5}(MoO_4)_2:Eu_{0.05}Yb_{0.45}$ caused the ratio of $Yb^{3+}:Eu^{3+}$ to be 9:1, while the lower intensity of (c) $LiY_{0.7}(MoO_4)_2:Eu_{0.1}Yb_{0.2}$ caused the ratio of $Yb^{3+}:Eu^{3+}$ to be 2:1. The optimal $Yb^{3+}:Eu^{3+}$ ratio was provided to be 9:1 induced by the concentration quenching effect of Eu^{3+} ion. Therefore, the higher content of the Yb^{3+} ion used as a sensitizer and lower content of the Eu^{3+} ion for the correct ratio of $Yb^{3+}:Eu^{3+}$ (9:1) can remarkably enhance the UC luminescence through the efficient energy transfer.

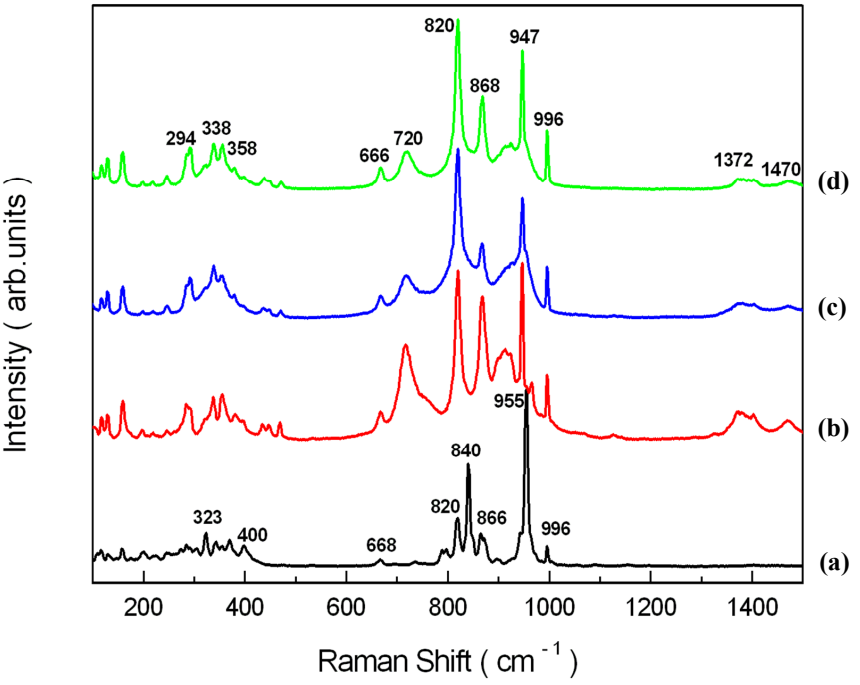

Figure 5: Raman spectra of the synthesized (a) $LiY(MoO_4)_2$, (b) $LiY_{0.8}(MoO_4)_2:Eu_{0.2}$, (c) $LiY_{0.7}(MoO_4)_2:Eu_{0.1}Yb_{0.2}$, and (d) $LiY_{0.5}(MoO_4)_2:Eu_{0.05}Yb_{0.45}$ particles excited by the 514.5-nm line of an Ar ion laser at 0.5 mW.

Fig. 5 provides the Raman spectroscopic results of the synthesized (a) $LiY(MoO_4)_2$, (b) $LiY_{0.5}(MoO_4)_2$:$Eu_{0.05}Yb_{0.45}$, (c) $LiY_{0.7}(MoO_4)_2$:$Eu_{0.1}Yb_{0.2,}$ and (d) $LiY_{0.5}(MoO_4)_2$:$Eu_{0.05}Yb_{0.45}$ phosphors excited by the 514.5-nm line of an Ar ion laser at 0.5 mW. The Raman spectra of the internal modes for the (a) $LiY(MoO_4)_2$ particles shows at 323, 400, 668, 820, 840, 866, 955 and 996 cm^{-1}, respectively. The well-resolved obvious peaks for the $LiY(MoO_4)_2$ particles provide a high crystallinity state of the synthesized phosphors. The internal vibration mode frequencies play an important role to identify the lattice parameters and the degree of the partially covalent bond between the cation and the molecular ionic group. The Raman spectra of the doped particles indicated the domination of strong peaks at higher frequencies of 666, 720, 820, 868, 947, and 996 cm^{-1} and the domination of weak peaks at lower frequencies of 294, 338 and 358 cm^{-1}. These strong disordered peaks at higher and lower frequencies are attributed to the formation of modulated structures of $LiY_{1-x}(MoO_4)_2$ by the incorporation of the Eu^{3+} and Yb^{3+} elements into the crystal lattice, which result in the unit cell shrinkage that accompanies the highly modulated MoO_{4-x} group [24,25]. However, the shape of the spectra recorded from the samples of doped Eu^{3+} differs strongly from that of the undoped sample. At this point, the shapes of all Eu-containing samples are very similar to each other and weakly vary with the Eu content, as well as with the presence of large contents of Yb. It is assumed that the highly modulated structure has strong absorption in the near ultraviolet region, so that energy transfer processes from the MoO_{4-x} group to rare earth ions can easily occur, which can greatly enhance the external quantum efficiency of rare earth ions doped materials. These results lead to high emitting efficiency and superior thermal and chemical stability, and these materials, which can overcome the current limitations of traditional photoluminescence materials, can be considered potentially active components in new optoelectronic devices and in luminescent imaging.

Conclusions

Eu^{3+}/Yb^{3+} co-doped $LiY_{1-x}(MoO_4)_2$ double molybdate phosphors with the correct doping concentrations of Eu^{3+} and Yb^{3+} (x = Eu^{3+} + Yb^{3+}, Er^{3+} = 0.05, 0.1, 0.2 and Yb^{3+}= 0.2, 0.45) were successfully synthesized via the microwave sol-gel route. The microstructure of the synthesized particles showed a well crystallized morphology with particle sizes of 2-10 μm. Under excitation at 980 nm, the UC $LiY_{0.5}(MoO_4)_2$:$Eu_{0.05}Yb_{0.45}$ particles showed a strong 525-nm emission band ($^7F_0 \rightarrow {}^5D_1$ transition) in the green region and a very weak 615-nm emission band ($^5D_0 \rightarrow {}^7F_2$ transition) in the red region. The optimal Yb^{3+}:Eu^{3+} ratio was provided to be 9:1 induced by the concentration quenching effect of Eu^{3+} ion. The Raman spectra of the doped particles indicated the domination of strong peaks at higher frequencies of 666, 720, 820, 868, 947, and 996 cm^{-1} and weak peaks at lower frequencies of 294, 338 and 358 cm^{-1}. The highly modulated structure of the doped samples were attributed to the strong mixing of stretching vibrations between the Mo-O bonds and the MoO_4 as well as the quenching effect of Eu^{3+} concentrations. These results led to high emitting efficiency and the involved materials can be considered potentially active components in new optoelectronic devices and in the field of luminescent imaging.

Acknowledgement

This research was supported by the Basic Science Research Program through the National Research Foundation of Korea (NRF) funded by the Ministry of Education (2015-058813).

References

[1] C.S. Lim, A. Aleksandrovsky, M. Molokeev, A. Oreshonkov, V. Atuchin, *Phys. Chem. Chem. Phys.* **17**, 19278 (2015).

[2] B. Yan, J.H. Wu, *Mater. Chem. Phys.,* **116**, 67 (2009).

[3] Y. Tian, X.H. Qi, X.W. Wu, R.N. Hua, B.J. Chen, *J. Phys. Chem.C*, **113**, 10767 (2009).

[4] C. Guo, H. K. Yang, J.H. Jeong, *J. Lumin*., **130**, 1390 (2010).

[5] J. Liao, D. Zhou, B. Yang, R. liu, Q. Zhang, Q. Zhou, *J. Lumin*., **134**, 533 (2013).

[6] J. Sun, J. Xian, H. Du, *J. Phys. Chem. Solids*, **72**, 207 (2011).

[7] T. Li, C. Guo, Y. Wu, L. Li, J.H. Jeong, *J. Alloys Comp*., **540**, 107 (2012).

[8] M. Nazarov, D.Y. Noh, *J. Rare Earths*, **28**, 1 (2010).

[9] J. Sun, W. Zhang, W. Zhang, H. Du, *Mater. Res. Bull*., **47**, 786 (2012).

[10] H. Du, Y. Lan, Z. Xia, J. Sun, *Mater. Res. Bull*., **44**, 1660 (2009).

[11] Z. Wang, H. Liang, M. Gong, Q. Su, *J. Alloys Comp*., **432**, 308 (2007).

[12] M. Haque, D.K. Kim, *Mater. Lett*., **63**, 793 (2009).

[13] C. Zhao, X. Yin, F. Huang, Y. Hang, *J. Solid State Chem*., **184**, 3190 (2011).

[14] L. Qin, Y. Huang, T, Tsuboi, H.J. Seo, *Mater. Res. Bull*., **47**, 4498 (2012).

[15] Y.L. Yang, X.M. Li, W.L. Feng, W.L. Li, C.Y. Tao, *J. Alloy Comp*., **505**, 239 (2010) .

[16] J. Yao, Z. Jia, P. Zhang, C. Shen, J. Wang, K.F. Aguey-Zinsou, C. Ma, L. Wang, *Ceram. Int*., **29**, 2165 (2013).

[17] Z. Xia, H. Du, J. Sun, D. Chen, X. Wang, *Mater. Chem. Phys*., **119**, 7 (2010).

[18] F. Wu, L. Wang, C. Wu, Y. Bai, *Electrochim. Acta*, 54, 4613 (2009)**.**

[19] C.S. Lim, *Mater. Chem. Phys*., **140**, 154 (2013).

[20] C.S. Lim, C.S. *Mater. Res. Bull*., **47**, 4220 (2013).

[21] Y. Huang, L. Zhou, L. Yang, Z. Tang, *Opt. Mater*., **32**, 777 (2011).

[22] J. Sun , J. Xian, X. Zhang, H. Du, *J. Rare Earths*, **29**, 32 (2011).

[23] Q. Sun, X. Chen, Z. Liu, F. Wang, Z. Jiang, C. Wang, *J. Alloys Comp*., **509**, 5336 (2012).

[24] C.S. Lim, *Mater. Res. Bull*., **48**, 3805 (2013).

[25] C.S. Lim, A. Aleksandrovsky, M. Molokeev, A. Oreshonkov, V. Atuchin, *J. Solid State Chem*., **228**, 160 (2015).